Inorg. Chem. **2003**, *42*, 2040–2048

Synthesis, Structure, and Spectroscopic, Photochemical, Redox, and Catalytic Properties of Ruthenium(II) Isomeric Complexes Containing Dimethyl Sulfoxide, Chloro, and the Dinucleating Bis(2-pyridyl)pyrazole Ligands

Cristina Sens, Montserrat Rodríguez, Isabel Romero, and Antoni Llobet*

Departament de Química, Universitat de Girona, Campus de Montilivi, E-17071 Girona, Spain

Teodor Parella

Departament de Química, Universitat Autònoma de Barcelona, Bellaterra, E-08193 Barcelona, Spain

B. Patrick Sullivan

Department of Chemistry, University of Wyoming, Laramie, Wyoming 82071-3838

Jordi Benet-Buchholz

BIS-ZAS X-ray Laboratory, Geb. Q18; Raum 490, Bayer AG, D-51368 Leverkusen, Germany

Received October 17, 2002

Two isomeric Ru(II) complexes containing the dinucleating Hbpp (3,5-bis(2-pyridyl)pyrazole) ligand together with Cl and dmso ligands have been prepared and their structural, spectroscopic, electrochemical, photochemical, and catalytic properties studied. The crystal structures of *trans,cis*-[$Ru^{II}Cl_2$(Hbpp)$(dmso)_2$], **2a,** and *cis(out),cis*-[$Ru^{II}Cl_2$-(Hbpp)$(dmso)_2$], **2b**, have been solved by means of single-crystal X-ray diffraction analysis showing a distorted octahedral geometry for the metal center where the dmso ligands coordinate through their S atom. 1D and 2D NMR spectroscopy corroborates a similar structure in solution for both isomers. Exposure of either **2a** or **2b** in acetonitrile solution under UV light produces a substitution of one dmso ligand by a solvent molecule generating the same product namely, *cis(out)*-[$Ru^{II}Cl_2$(Hbpp)(MeCN)(dmso)], **4**. While the 1 e^- oxidation of **2b** or *cis(out),-cis*-[$Ru^{II}Cl_2$(bpp)$(dmso)_2]^+$, **3b**, generates a stable product, the same process for **2a** or *trans,cis*-[$Ru^{II}Cl_2$(bpp)$(dmso)_2]^+$, **3a**, produces the interesting linkage isomerization phenomenon where the dmso ligand switches its bond from Ru–S to Ru–O ($K^{III}_{O\rightarrow S} = 0.25 \pm 0.025$, $k^{III}_{O\rightarrow S} = 0.017\ s^{-1}$, and $k^{III}_{S\rightarrow O} = 0.065\ s^{-1}$; $K^{II}_{O\rightarrow S} = 6.45 \times 10^9$, $k^{II}_{O\rightarrow S} = 0.132\ s^{-1}$, $k^{II}_{S\rightarrow O} = 2.1 \times 10^{-11}\ s^{-1}$). Finally complex **3a** presents a relatively high activity as hydrogen transfer catalyst, with regard to its ability to transform acetophenone into 2-phenylethyl alcohol using 2-propanol as the source of hydrogen atoms.

Introduction

Ruthenium complexes are gathering a great deal of attention because of their multiple applications in many fields of science. They are being used extensively as catalyst for a myriad of different process including oxidative and reductive reactions[1] and recently as molecular machine type of devices.[2]

From a bioinorganic perspective, they are being utilized as probes for understanding electron-transfer processes and oxidations in DNA.[3] Furthermore, since the discovery of the anticancer activity of [$RuCl_2(dmso)_4$], several ruthenium−dmso complexes have been studied as antitumoral drugs and the mechanism and scope of their applications is being

* To whom correspondence should be addressed. E-mail: antoni.llobet@udg.es.

10.1021/ic026114o CCC: $25.00
Published on Web 02/28/2003

studied at present.[4] They have also been described as molecular switching devices with regard to their capacity to switch on or off the rotation of a neighboring ligand.[5] In addition, they are also of interest because of the ability of the Ru−dmso bond to undergo linkage isomerism and the implications this reaction has from the perspective of using them as molecular memories.[6]

Furthermore, properly designed dinucleating ligands can form dinuclear metal complexes that can generate metal−metal cooperative effects leading to genuine reactivity patterns.[7,8]

In this report we present the synthesis, characterization, and chemical properties of isomeric Ru−dmso complexes containing the dinucleating 3,5-bis(2-pyridyl)pyrazole (Hbpp) ligand, of general formula $[RuCl_2(Hbpp)(dmso)_2]$. This ligand

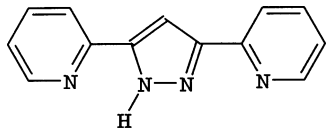

Hbpp

is also of interest because its mononuclear complexes have a free pyridyl ring that can generate π-stacking interactions and because they can be used as starting materials to generate both homo- and heterodinuclear complexes where the metal sites are strategically situated in close proximity.

Experimental Section

Materials. All reagents used in this work were obtained from Aldrich Chemical Co. and were used without further purification. Reagent grade organic solvents were obtained from SDS, and high-purity deionized water was obtained by passing distilled water through a nano-pure Mili-Q water purification system. $RuCl_3 \cdot 2H_2O$, was supplied by Johnson and Matthey Ltd. and was used as received.

Preparations. $[RuCl_2(dmso_4)]$[9] and the Hbpp[10] ligand were prepared according to literature procedures. All synthetic manipulations were routinely performed under nitrogen atmosphere using Schlenck tubes and vacuum line techniques. Electrochemical experiments were performed under N_2 atmosphere with degassed solvents. All spectroscopic, electrochemical, and synthetic experiments were performed in the absence of light unless explicitly mentioned.

***trans,cis*-[$Ru^{II}Cl_2$(Hbpp)(dmso)$_2$], 2a.** A 0.14 g (0.63 mmol) sample of Hbpp and 0.3 g (0.62 mmol) of $[RuCl_2(dmso)_4]$ were dissolved in 20 mL of methanol, and the resulting solution refluxed for 45 min. A light orange solid was formed and was filtered on a frit, washed with ether, and vacuum-dried. Yield: 189 mg (55.5%). Anal. Found (calcd) for $C_{17}H_{23}Cl_2N_4O_{2.5}RuS_2$; C, 36.5 (36.5); H, 4.1 (4.1); N, 9.7 (10.0); S, 11.4 (11.5). ^{1}H NMR ($CDCl_3$, 500 MHz; δ): 8.69 (d, $J_{13-12} = 3.5$ Hz, H13), 8.52 (d, $J_{12} = 4.5$ Hz, H1), 7.95 (d, $J_{43} = 7$ Hz, H4), 7.89 (dd, $J_{32} = 6.5$ Hz, H3), 7.80 (dd, $J_{11-12} = 6$ Hz, $J_{11-10} = 7.5$ Hz, H11), 7.68 (d, H10), 7.44 (s, H7), 7.36 (dd, H2), 7.31 (dd, H12), 3.65 (s, CH_3 of C14 and C15), 3.57 (s, CH_3 of C16 and C17). ^{13}C NMR ($CDCl_3$; δ): 152.1 (C1), 124.4 (C2), 138.3 (C3), 122.5 (C4), 102.6 (C7), 120.4 (C10), 137.9 (C11), 124.4 (C12), 150.5 (C13), 43.1 (C14, C15), 45.6 (C16, C17). For the NMR assignments we use the same labeling scheme as for the X-ray structures (Figure 1).

***cis(out),cis*-[$Ru^{II}Cl_2$(Hbpp)(dmso)$_2$], 2b.** This complex was prepared in manner identical to the case for **2a** except that the reflux was performed overnight. A yellow solid was obtained. Yield: 0.271 g (75.3%; obtained from 0.317 g (0.65 mmol) of $[RuCl_2(dmso)_4]$). Anal. Found (calcd) for $C_{17}H_{24.6}Cl_2N_4O_{3.3}RuS_2$; C, 35.4 (35.6); H, 4.1 (4.3); N, 9.5 (9.8); S, 10.9 (11.2). ^{1}H NMR ($CDCl_3$, 500 MHz; δ): 9.54 (d, $J_{12} = 5.25$ Hz, H1), 8.69 (d, $J_{12-13} = 3.85$ Hz, H13), 8.0 (dd, $J_{23} = 7$ Hz, $J_{34} = 8.05$ Hz, H3), 7.97 (dd, H4), 7.93 (dd, $J_{11-12} = 8.4$ Hz, $J_{11-10} = 7.15$ Hz, H11), 7.72 (d, H10), 7.71 (s, H7), 7.50 (dd, H2), 7.42 (dd, H12), 3.71 (s, CH_3 of C15), 3.69 (s, CH_3 of C14), 3.14 (s, CH_3 of C16), 2.14 (s, CH_3 of C17). ^{13}C NMR ($CDCl_3$; δ): 152.0 (C1), 124.9 (C2), 139 (C3), 122.1 (C4), 104.0 (C7), 120.6 (C10), 139 (C11), 124.6 (C12), 148.2 (C13), 45.0 (C14, C15), 45.4 (C16), 43.7 (C17).

***cis(out)*-[$Ru^{II}Cl_2$(Hbpp)(MeCN)(dmso)], 4.** This compound was obtained from a solution of **2a** or **2b** in acetonitrile after 4 h of irradiation using a 254 nm 80 W UV lamp source.

Instrumentation and Measurements. IR spectra were recorded on a Mattson Satellite FT-IR with KBr pellets. UV−vis spectroscopy was performed on a Cary 50 Scan (Varian) UV−vis spectrophotometer with 1 cm quartz cells or with an immersion probe of 5 mm path length. Cyclic voltammetric (CV) experiments were performed in an IJ-Cambria IH-660 potentiostat using a three electrode cell. A platinum disk electrode (2 mm diameter) was used as working electrode, platinum wire as auxiliary electrode, and SSCE as the reference electrode. All cyclic voltammograms presented in this work were recorded in the absence of light under nitrogen atmosphere unless explicitly mentioned. The complexes

(1) (a) Murahashi, S.-I.; Takaya, H.; Naota, T. *Pure Appl. Chem.* **2002**, *74*, 19. (b) Naota, T.; Takaya, H.; Murahashi, S.-I. *Chem. Rev.* **1998**, *98*, 2599. (c) Riley, D. P.; Oliver, J. D. *Inorg. Chem.* **1996**, *25*, 1825. (d) Rodríguez, M.; Romero, I.; Llobet, A.; Deronzier, A.; Biner, M.; Parella, T.; Soteckli-Evans, H. *Inorg. Chem.* **2001**, *40*, 4150. (e) Chronister, C. W.; Binstead, R. A.; Ni, J.; Meyer, T. J. *Inorg. Chem.* **1997**, *36*, 3814. (f) Jauregui-Haza, U. J.; Dessoudeix, M.; Kalck, P.; Wilhelm, A. M.; Delmas, H. *Catal. Today* **2001**, *66*, 297.

(2) (a) Ballardini, R.; Balzani, V.; Credi, A.; Gandolfi, M. T.; Venturi, M. *Int. J. Photoenergy* **2001**, *3*, 63. (b) Ashton, P. R.; Ballardini, R.; Balzani, V.; Credi, A.; Dress, K. R.; Ishow, E.; Kleverlaan, C. J.; Kocian, O.; Preece, J. A.; Spencer, N.; Stoddart, J. F.; Venturi, M.; Wenger, S. *Chem.—Eur. J.* **2000**, *6*, 3558. (c) Baranoff, E.; Collin, J.-P.; Furusho, J.; Furusho, Y.; Laemmel, A.-C.; Sauvage, J.-P. *Inorg. Chem.* **2002**, *41*, 1215.

(3) (a) Weatherly, S. C.; Yang, I. V.; Thorp, H. H. *J. Am. Chem. Soc.* **2001**, *123*, 1236. (b) Kelly, S. O.; Barton, J. K. *Science* **1999**, *238*, 375. (c) Hall, D. B.; Holmlin, R. E.; Barton. J. K. *Nature* **1996**, *384*, 731. (d) Burrows, C. J.; Muller, J. G. *Chem. Rev.* **1998**, *98*, 1109. (e) Schuster, G. B. *Acc. Chem. Res.* **2000**, *33*, 253.

(4) (a) Malina, J.; Novakova, O.; Keppler, B. K.; Alessio, E.; Bravec, B. *J. Biol. Inorg. Chem.* **2001**, *6*, 435. (b) Clark, M. J.; Zhu, F.; Frasca, D. R. *Chem. Rev.* **1999**, *99*, 2511.

(5) Iwamoto, M.; Alessio, E.; Marzilli, L. G. *Inorg. Chem.* **1996**, *35*, 2384.

(6) (a) Tomita, A.; Sano, M. *Chem. Lett.* **1996**, 981. (b) Sano, M.; Taube, H. *J. Am. Chem. Soc.* **1991**, *113*, 2327. (c) Tomita, A.; Sano, M. *Inorg. Chem.* **2000**, *39*, 200. (d) Sano, M.; Sago, H.; Tomita, A. *Bull. Chem. Soc. Jpn.* **1996**, *69*, 977. (e) Sano, M. *Inorg. Chem.* **1994**, *33*, 705.

(7) (a) Fraser, C.; Ostrander, R.; Rheingold, A.; White, C.; Bosnich, B. *Inorg. Chem.* **1994**, *33*, 324. (b) Di Pietro, C.; Serroni, S.; Campagna, S.; Gandolfi, M. T.; Ballardini, R.; Fanni, S.; Browne, W. R.; Vos, J. G. *Inorg. Chem.* **2002**, *41*, 2871. (c) Bartolotti, L. J.; Pedersen, L. G.; Meyer, T. J. *Int. J. Quantum Chem.* **2001**, *83*, 143.

(8) (a) Catalano, V. J.; Heck, R. A.; Ohman, A.; Hill, M. G. *Polyhedron* **2000**, *19*, 1049. (b) Catalano, V. J.; Heck, R. A.; Immoos, C. E.; Robinson, A.; Hill, M. G. *Inorg. Chem.* **1998**, *37*, 2150.

(9) Evans, I. P.; Spencer, A.; Wilkinson, J. *J. Chem. Soc., Dalton Trans.* **1973**, *2*, 204.

(10) (a) Levine, R.; Sneed, J. K. *J. Am. Chem. Soc.* **1951**, *73*, 5614. (b) Teixidor, F.; Garcia, R.; Pons, J.; Casabó, J. *Polyhedron* **1998**, *7*, 43. (c) Casabo, J.; Pons, J.; Siddiqi, K. S.; Teixidor, F.; Molins, E.; Miravitlles, C. *J. Chem. Soc., Dalton Trans.* **1989**, 1401. (d) Pons, J.; Sanchez, F. J.; Lopez, X.; Teixidor, F.; Casabo, J. *Polyhedron* **1990**, *9*, 2839.

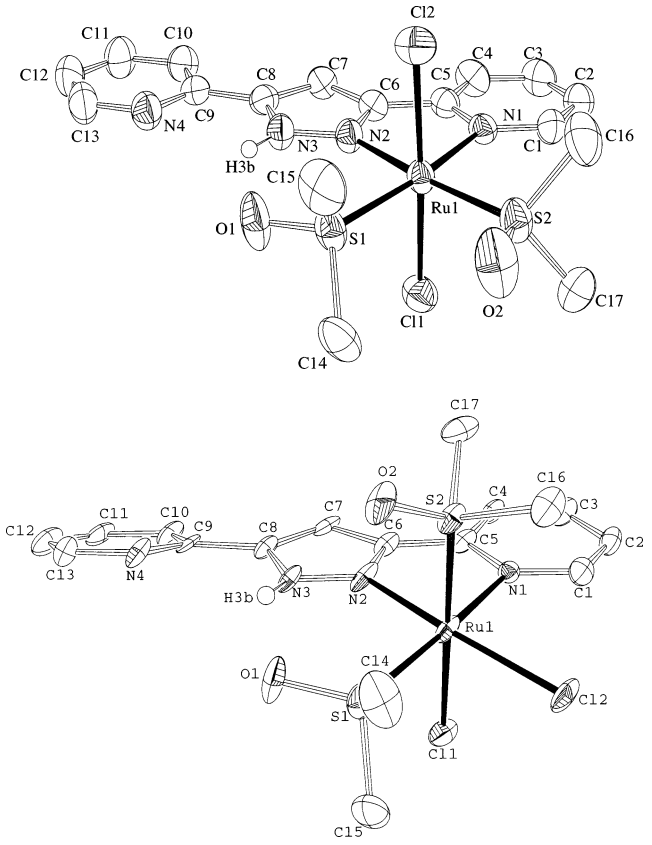

Figure 1. X-ray structures (Ortep plots with ellipsoids at 50% probability level) and labeling scheme for **2a** (top) and **2b** (bottom).

were dissolved in previously degassed solvents containing the necessary amount of n-$Bu_4N^+PF_6^-$ (TBAH) as supporting electrolyte to yield a 0.1 M ionic strength solution. All $E_{1/2}$ values reported in this work were estimated from cyclic voltammetric experiments as the average of the oxidative and reductive peak potentials ($E_{p,a} + E_{p,c}$)/2. Unless explicitly mentioned the concentration of the complexes was approximately 1 mM. The ^{1}H NMR spectroscopy was performed on a Bruker DPX 200 MHz or a Bruker 500 MHz. Samples were run in $CDCl_3$ or acetonitrile-d_3 with internal references (residual protons and/or tetramethylsilane). Elemental analyses were performed using a CHNS-O EA-1108 elemental analyzer from Fisons. Monochromatic irradiations were carried out by using a 254 nm 80 W UV lamp source from Phillips on complex solutions, typically 1 mM. To determine the pseudo-first-order kinetic constants of the photochemical reactions, a total of 109 spectra in the range of 290−520 nm were recorded for each experiment at a constant temperature of 22.0 ± 0.1 °C. A spectrum was recorded each 0.5 min during the first 30 min of the reactions, each 1 min during the following 60 min, and each 5 min for the last 150 min. Kinetic data treatment was performed using Specfit Program from Spectrum Software Ass. Gas chromatography experiments were performed by capillary GC, using a GC-17A gas chromatograph from Shimadzu, equipped with a J&W Scientific β-cyclodex chiral column. All the product analysis in the catalytic experiments were performed by means of GC experiments with calibrated authentic samples using biphenyl as internal standard.

X-ray Structure Determination. Suitable crystals of *trans,cis*-[$RuCl_2$(Hbpp)(dmso)$_2$], **2a**, were grown from methanol as small orange cubes. Crystals of *cis*(*out*),*cis*-[$RuCl_2$(Hbpp)(dmso)$_2$], **2b**, were obtained by slow diffusion of diethyl ether into a dichloromethane solution of the complex, yielding in the best case to yellow needles of very small size and bad quality. After different trials, a data set of moderate quality could be acquired from **2b** (crystal dimensions: 340 × 12 × 8 μm^3) using a extreme long measuring time and high X-ray intensity.

***trans,cis*-[$RuCl_2$(Hbpp)(dmso)$_2$], 2a. Data Collection**. The measurement in the range 1.65−27.50° was made on a Siemens P4 diffractometer equipped with a molybdenum tube and a graphite monochromator at 298 K. A total of 5779 reflections were collected of which 5507 are unique (R_{int} = 0.0233). Unit-cell dimensions were determined from several accurately centered reflections using XSCANS. Data collection and processing with XSCANS (Siemens, Ver. 2.31, 1997).[11]

Structure Solution and Refinement. SHELXTL Version 2.31 (Sheldrick, 1997) was used;[12] structure solution was with Patterson methods.

***cis,cis(out)*-[$RuCl_2$(Hbpp)(dmso)$_2$], 2b. Data Collection**. Measurements were made on a Siemens P4 diffractometer equipped with a SMART-CCD-1000 area detector, a MACScience Co. rotating anode with Mo Kα radiation, a graphite monochromator, and a Siemens LT2 low-temperature device (T = −120 °C). The measurements were made in the range 1.65−30.07°. A total of 12 761 reflections were collected of which 4753 are unique (R_{int} = 0.0654). Full-sphere data collection was used with ω and φ scans. Programs used: data collection, Smart V. 5.060 (BrukerAXS 1999); data reduction, Saint + Version 6.02 (Bruker AXS 1999); absorption correction, SADABS (Bruker AXS 1999).

Structure Solution and Refinement. SHELXTL Version 5.10 (Sheldrick, 1998) was used.

Results and Discussion

Synthesis, Structure, and Stereoisomerism. Reaction of equimolecular amounts of [$RuCl_2$(dmso)$_4$], **1**, and the neutral Hbpp ligand in methanol at reflux for 45 min under nitrogen produces the *trans*-Cl, *cis*-dmso **2a** complex in good yield,

$$\underset{\mathbf{1}}{[RuCl_2(dmso)_4]} + Hbpp \rightarrow \underset{\mathbf{2a}}{trans,cis\text{-}[RuCl_2(Hbpp)(dmso)_2]} \quad (1)$$

Similar results are obtained in the literature[13] for the same reaction but using two different unsymmetric didentate ligands.

If in the previous reaction the reflux process is extended up to 15 h, then only the *cis*-Cl, *cis*-dmso complex **2b** is obtained in 75% yield. Thus, the following isomerization process is occurring:

$$\underset{\mathbf{2a}}{trans,cis\text{-}[RuCl_2(Hbpp)(dmso)_2]} \xrightarrow{15\text{ h reflux}} \underset{\mathbf{2b}}{cis(out),cis\text{-}[RuCl_2(Hbpp)(dmso)_2]} \quad (2)$$

The substitution of two dmso ligands in **1** by an unsymmetric NN′ ligand such as Hbpp can potentially lead to six different

(11) *Siemens XSCANS Ver. 2.31*; Siemens Energy and Automation, Inc.: Madison, WI, 1997.
(12) Sheldrick, G. M. *SHELXTL Crystallographic System Ver. 5.10*; Siemens Analytical X-ray Instruments, Inc.: Madison, WI, 1997.
(13) (a) Cingi, M. B.; Lanfranchi, M.; Pellinghelli, M. A.; Tegoni, M.*Eur. J. Inorg. Chem.* **2000**, 703. (b) Alessio, E.; Calligaris, M.; Iwamoto, M.; Marzilli L. G. *Inorg. Chem.* **1996**, *35*, 2538.

Scheme 1. Possible Stereoisomers for $[RuCl_2(Hbpp)(dmso)_2]$ (Enantiomers Not Shown)

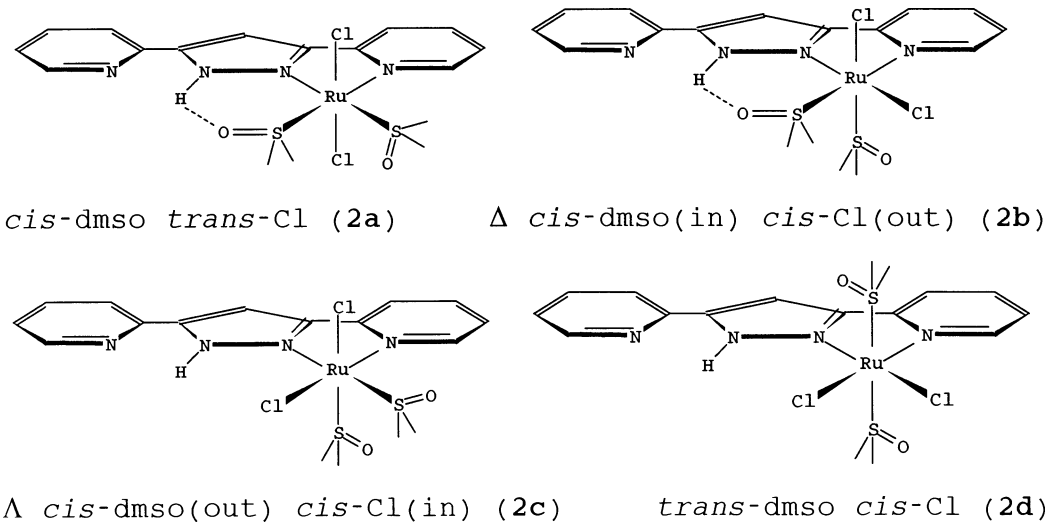

stereoisomers, including two pairs of enantiomers, as depicted in Scheme 1.

From here on, the equatorial plane of the complex is taken as the plane that would ideally contain the Hbpp ligand. The term *in* and *out* is used to indicate whether another equatorial ligand is directed toward or away, respectively, from the Hbpp center.

The fact that only one isomer is obtained in this type of reactions is indicative that **2a** is the kinetically favored isomer. The five stereoisomers can be potentially obtained using **2a** as the starting material. In sharp contrast the isomerization process indicated in reaction 2 yields only one pair of enantiomers (Λ-**2b** and Δ-**2b**). These results can be rationalized taking into account the following structural and electronic factors: (a) Ru(II) is a d^6 ion, it forms strong bonds with pyridylic ligands, and they do not exchange in solution with other coordinated ligands.[1d,14] (b) The existance of a strong hydrogen bonding between the oxygen atom of the inner coordinated dmso ligand with the N-bonded pyrazolylic hydrogen atom (see below in the X-ray structure). (c) Synergistic π-donor and π-acceptor effects among the Cl and dmso ligands, respectively. (d) Unfavorable steric effects produced by dmso ligands in the cis position.[15]

The mentioned hydrogen bonding in **2a** (vide infra) produces an extra stabilization of the inner dmso with regard to the outer one. As a consequence of this, the synchronous interconversion motion of the outer dmso ligand and one of the Cl ligands easily generates the **2b** pair of enantiomers with the equatorial Cl in the outer position. Further, the **2b** isomers are assumed to be thermodynamically more stable than **2a** on the basis of trans influence[16] and the synthetic evidence presented in this work. The formation of the pair of enantiomers **2c** is a more energetically demanding reaction since it requires initially the breaking of hydrogen bonding and then the positional interchange of Cl and now the inner dmso ligand. Finally, the formation of **2d** requires a larger ligand rearrangement and the formation of the less favorable *trans*-dmso array, due to π-back-bonding competition.

Table 1. Crystal Data for Complexes *trans*,*cis*-$[RuCl_2(Hbpp)(dmso)_2]$, **2a**, and *cis*,*cis*-$[RuCl_2(Hbpp)(dmso)_2]$, **2b**

	2a	**2b**
empirical formula	$C_{18}H_{26}Cl_2N_4O_3RuS_2$	$C_{17}H_{23}Cl_2N_4O_{3.34}RuS_2$
fw	582.52	572.84
cryst system, space group	monoclinic, $P2_1/c$	triclinic, $P\bar{1}$
a, Å	11.186(2)	7.9528(13)
b, Å	13.902(3)	11.4298(19)
c, Å	15.629(3)	12.618(2)
α, deg	90.00	86.819(6)
β, deg	99.38(3)	78.509(7)
γ, deg	90.00	88.796(7)
V, Å^3	2397.9(8)	1122.2(3)
formula units/cell	4	2
temp, K	298(2)	153(2)
λ(Mo Kα), Å	0.710 73	0.710 73
ρ_{calc}, g cm^{-3}	1.614	1.695
μ, mm^{-1}	1.077	1.151
R_1[a]	0.0338	0.0891
wR_2[b]	0.0766	0.2149

[a] $R_1 = \sum||F_o| - |F_c||/\sum|F_o|$. [b] $wR_2 = [\sum\{w(F_o^2 - F_c^2)^2\}/\sum\{w(F_o^2)^2\}]^{1/2}$, where $w = 1/[\sigma^2F_o^2 + (0.0377P)^2 + 1.65P]$ and $P = (F_o^2 + 2F_c^2)/3$.

Crystallographic data and selected bond distances and angles for complexes **2a,b** are presented in Tables 1 and 2, respectively; ORTEP views together with their labeling schemes are depicted in Figure 1. In complex **2a** the Ru metal center adopts a pseudooctahedral geometry where the trans Cl ligands can be regarded as occupying the axial positions (Cl(1)−Ru(1)−Cl(2) angle is 175.18(3)°). The metal−ligand bonding distances are unremarkable and similar to related complexes previously described in the literature for Ru(II).[15−17] In contrast, bonding angles are interesting since they reflect the chosen ligand arrangement around the ruthenium metal center. Both Cl ligands are tilted 2−3° toward the plane formed by the Hbpp ligand avoiding the steric effects provoked by the methyl groups of the dmso ligands. The

(14) Romero, I.; Rodríguez, M.; Llobet, A.; Collomb-Dunand-Sauthier, M.; Deronzier, A.; Parella, T.; Stoeckli-Evans, H. *J. Chem. Soc., Dalton Trans.* **2000**, 1689.
(15) Alessio, E.; Mestroni, G.; Nardin, G.; Attia, W. M.; Calligaris, M.; Sava, G.; Zorzet, S. *Inorg. Chem.* **1988**, *27*, 4099.
(16) Calligaris, M.; Carugo, O. *Coord. Chem. Rev.* **1996**, *153*, 83.
(17) Laurent, F.; Plantalech, E.; Donnadieu, B.; Jiménez, A.; Hernández, F.; Martínez-Ripoll, M.; Biner, M.; Llobet, A. *Polyhedron* **1999**, *18*, 3321.

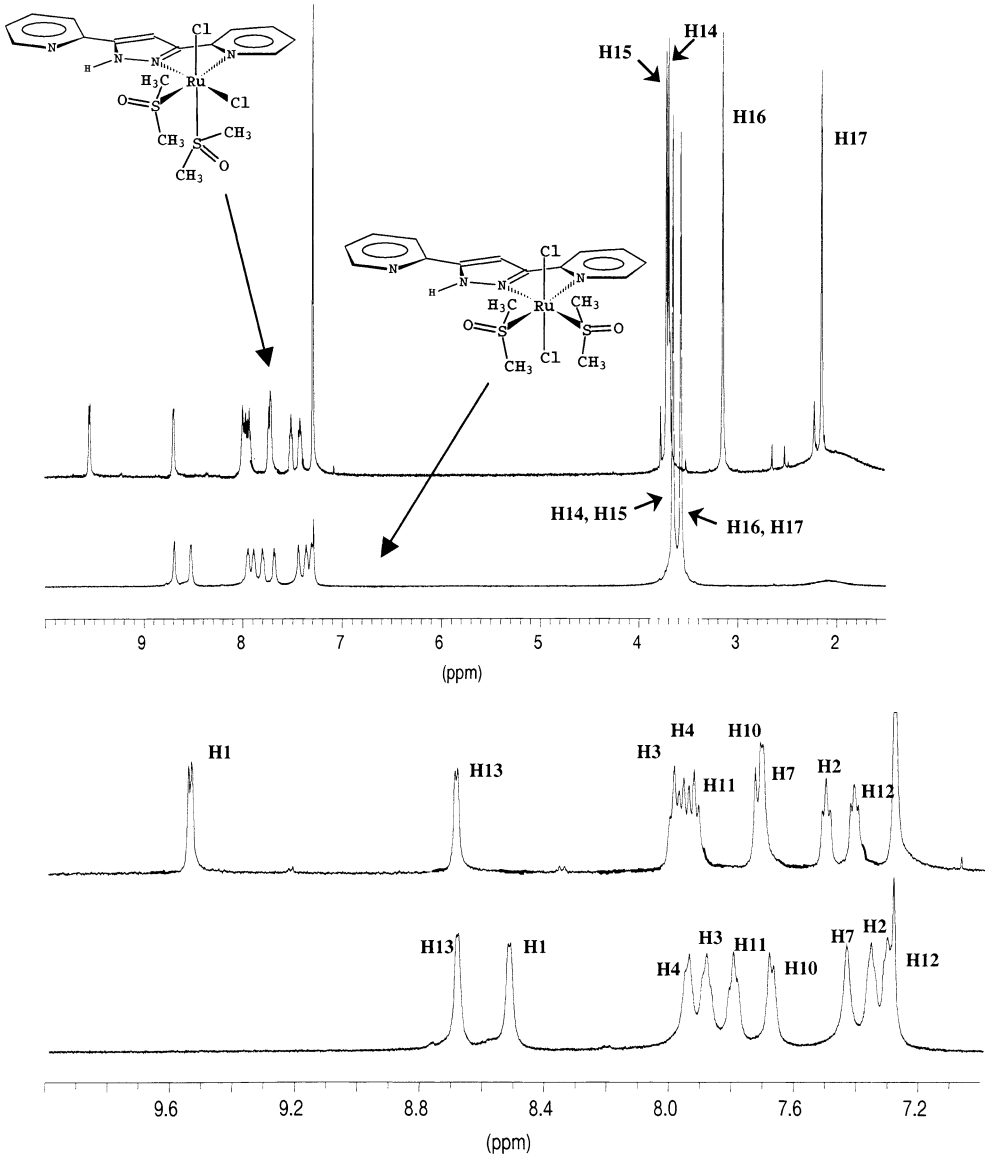

Figure 2. ^{1}H NMR spectra in $CDCl_3$ for complexes **2a** (bottom) and **2b** (top).

N(1)−Ru(1)−N(2) angle is of only 76.27(10)°, showing the geometrical restrictions imposed by Hbpp acting as a chelator ligand. As a consequence of this, the rest of the equatorial cis angles are larger than the 90° expected for an ideal octahedral geometry. The strong hydrogen bonding between the oxygen atom of the inner dmso ligand and the hydrogen atom of the pyrazole group[18] (hydrogen bonding parameters: H(3b)−O(1) = 1.98(5) Å, N(3)−O(1) = 2.685(4) Å, and N(3)−H(3b)−O(1) = 133(5)°) produces a relatively small N(2)−Ru(1)−S(1) angle of 92.40(7)° with the methyl groups situated below and above the plane described by the Hbpp ligand. As a result of this methyl arrangement the outer dmso ligand adopts a conformation with the methyl groups also above and below the Hbpp plane, as in the previous case but with the methyl groups oriented outward. This generates the larger equatorial cis angle of 98.75(7)° for N(1)−Ru(1)−S(2) due to the steric effects between the mentioned methyl groups and the coordinated Hbpp pyridylic group. This pyridyl group is rotated 0.8° with regard to the central pyrazolylic group whereas the noncoordinated pyridyl group is rotated only by 3.1(5)° (N(4)−C(9)−C(8)−N(3)). This small rotation, compared to related complexes where the analogous rotation can be up to 180°, is due to the hydrogen bonding between N(4) and H(3b) (2.49(5) Å), the pyrazolylic hydrogen atom bonded to N(3).

In complex **2b** the Ru metal center adopts a pseudooctahedral geometry with ruthenium bonding distances relatively similar to those of **2a**. The bonding angles vary slightly, especially due to the fact that now there is only one bulky dmso ligand that remains in the equatorial plane (the plane formed by the atoms N(1)−N(2)−Ru(1)−S(1)−Cl(2)). Thus, the N(1)−Ru(1)−Cl(2) angle is reduced by approximately 3° to 95.2(2)° and as a consequence the N(2)−Ru(1)−S(1) angle increases about 3° to 95.6(3)°. Complex **2b** also displays strong hydrogen bonding between the oxygen atom of the equatorial dmso and the pyrazolylic hydrogen atom (H(3b)−O(1) = 2.08(12) Å, N(3)−O(1) = 2.826(12) Å, and N(3)−H(3b)−O(1) = 143(11) Å). A significant difference

(18) Anda, C.; Llobet, A.; Salvadó, V.; Motekaitis, R.; Riebenspies, J.; Martell, A. E. *Inorg. Chem.* **2000**, *39*, 2986.

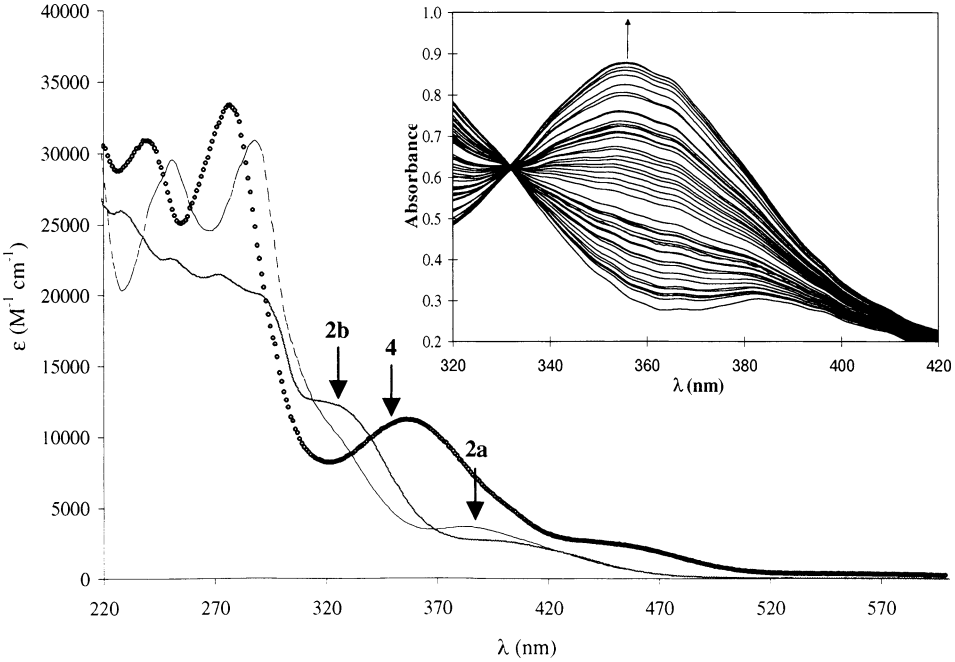

Figure 3. UV−vis spectroscopy of **2a,b** and **4**. The inset shows the photochemical transformation of **2a** into **4** in the 320−420 nm range. (For details see the Experimental Section.)

from the previously described structure is the increase of 14.4° in the tilting angle of the free pyridyl ring with regard to the plane formed by the bonded aromatic rings up to 17.5-(13)°.

Spectroscopic and Photochemical Properties. The ^{1}H NMR spectra of the complexes described in this work were recorded in $CDCl_3$ or acetonitrile-d_3 and are assigned in the Experimental Section. Figure 2 shows the ^{1}H NMR spectra of **2a,b**; the corresponding 2D NMR spectra are presented as Supporting Information. All resonances in Figure 2 can be unambiguously assigned by taking into account the symmetry of the molecule and the integrals and by examining the 2D NMR spectra.[19]

Both complexes exhibit two set of signals: one in the aromatic region due to the Hbpp ligand; the other in the aliphatic region due to the methyl groups of the bonded dmso ligands. In solution complex **2a** possesses a plane of symmetry that contains Hbpp and bisects the dmso ligands, even though it rigorously does not exist in the solid state (vide supra), thus reducing the complexity of the spectra in the aliphatic region. The NOESY effect observed between H1 and C16−C17 allows one to identify the "out" dmso ligand and the metal-bonded pyridyl ring of the Hbpp ligand. The rest of the resonances are then easily identified through the COSY spectrum.

In complex **2b** the deshielding effect produced by the equatorial Cl ligand to the H1[1d] allows one to identify the bonded pyridyl group and then, again as in the previous case, the COSY spectrum permits one to fully assign the resonances of the aromatic region. Complex **2b** is an asymmetric molecule, and therefore, it generates 4 different methyl resonances due to the dmso ligands. The anisotropic effect of the aromatic ligand over the C17 methyl and the NOE effect observed between H1 and the C16 methyl allows one to clearly identify the two resonances of the axial dmso ligand. On the other hand, the methyl resonances of the equatorial dmso ligand can be tentatively assigned on the basis of the stronger deshielding effect of the axial Cl ligand over the C15 than the C14 methyl group.

As expected for d^6-Ru(II) complexes, their solution structures are consistent with their corresponding solid-state structures.

UV−vis spectra for complexes **2a,b** and **4** are depicted in Figure 3, and their more prominent spectral features together with those of the free ligand, Hbpp, are summarized in Table 3. The bands appearing at wavelength values above 300 nm can be assigned to $d\pi \rightarrow \pi^*$ (Ru → Hbpp) on the basis of the similarity of their transition energy and extinction coefficients with related complexes.[8,20] As expected, the absorptions for the cis and trans isomers **2a,b** are relatively similar whereas a low-energy shift is observed for complex **4**. The removal of a soft S-bounded dmso ligand by stronger σ donor ligand like MeCN provokes a destabilization of the $d\pi$(Ru) donor orbital whereas the π^*(Hbpp) remain virtually unchanged. As a consequence of this, the energy gap for the $(d\pi)^6$ ground state and the $(d\pi)^5(\pi^*)^1$ excited states decreases.

The color of the acetonitrile solutions of **2a,b** changes from light to deep yellow after exposition to UV or sun light for a few minutes, indicating the occurrence of light-induced processes. To follow the process a 254 nm UV lamp was used to irradiate the complexes and the spectrophotometric changes were monitored using a UV−vis apparatus at 22.0 ± 0.1 °C. In both cases the UV−vis spectra showed

(19) Ravindar, V.; Lingaiah, P.; Reddy, K. V. *Inorg. Chim. Acta* **1984**, *87*, 35.

(20) (a) Llobet, A. *Inorg. Chim. Acta* **1994**, *221*, 125. (b) Barqawi, K., *Llobet, A.*, Meyer, T. J. *J. Am. Chem. Soc.* **1988**, *110*, 7751.

Table 2. Selected Bond Lengths (Å) and Angles (deg) for **2a,b**

	2a	**2b**
Ru(1)−N(1)	2.171(2)	2.120(8)
Ru(1)−N(2)	2.061(2)	2.034(8)
Ru(1)−S(1)	2.2672(9)	2.249(3)
Ru(1)−S(2)	2.2773(9)	2.236(2)
Ru(1)−Cl(1)	2.3954(10)	2.430(2)
Ru(1)−Cl(2)	2.4113(10)	2.409(2)
O(1)−N(3)	2.685(4)	2.826(12)
O(1)−H(3b)	1.980(5)	2.080(12)
N(1)−Ru(1)−N(2)	76.270(10)	77.50(3)
N(1)−Ru(1)−S(1)	168.30(7)	171.20(2)
N(1)−Ru(1)−S(2)	98.75(7)	93.50(2)
N(1)−Ru(1)−Cl(1)	87.58(7)	83.20(2)
N(1)−Ru(1)−Cl(2)	90.64(7)	95.20(2)
N(2)−Ru(1)−S(1)	92.40(7)	95.60(3)
N(2)−Ru(1)−S(2)	174.92(7)	90.60(2)
N(2)−Ru(1)−Cl(1)	87.52(8)	86.80(2)
N(2)−Ru(1)−Cl(2)	87.71(8)	172.00(3)
S(1)−Ru(1)−S(2)	92.63(4)	92.190(11)
S(1)−Ru(1)−Cl(1)	89.03(3)	90.820(11)
S(1)−Ru(1)−Cl(2)	91.84(3)	91.310(10)
S(2)−Ru(1)−Cl(1)	93.29(4)	176.150(11)
S(2)−Ru(1)−Cl(2)	91.40(3)	93.160(10)
Cl(1)−Ru(1)−Cl(2)	175.18(3)	89.160(9)
N(3)−H(3b)−O(1)	133.00(5)	143.00(11)
N(1)−C(5)−C(6)−N(2)	2.20(4)	0.800(13)
N(3)−C(8)−C(9)−N(4)	3.10(5)	17.500(13)

Table 3. UV−Vis Spectral Features for the Hbpp Ligand and for Complexes **2a,b** and **4**

compd	solvent	λ_{max} (nm)	ϵ (M^{-1} cm^{-1})	assgnt
Hbpp	MeOH	245	56 238	$\pi-\pi^*$
		285	49 505	$\pi-\pi^*$
trans,cis-[$RuCl_2$(Hbpp)(dmso)$_2$] (**2a**)	CH_3CN	251	29 541	$\pi-\pi^*$
		288	30 917	$\pi-\pi^*$
		326	9 963	d$\pi-\pi^*$
		385	3 688	d$\pi-\pi^*$
cis,cis-[$RuCl_2$(Hbpp)(dmso)$_2$] (**2b**)	CH_3CN	228	26 062	$\pi-\pi^*$
		251	22 622	$\pi-\pi^*$
		272	21 469	$\pi-\pi^*$
		287	20 196	$\pi-\pi^*$
		321	12 446	d$\pi-\pi^*$
		392	2 718	d$\pi-\pi^*$
cis(*out*)-[$RuCl_2$(Hbpp)(CH_3CN)(dmso)] (4)	CH_3CN	238	30 899	$\pi-\pi^*$
		277	33 394	$\pi-\pi^*$
		356	11 229	d$\pi-\pi^*$
		448	2 495	d$\pi-\pi^*$

isosbestic points (247, 259 283, and 330 nm for **2a**; 230, 249, 259, 288, and 340 nm for **2b**) leading to exactly the same spectra, forming presumably the complex *cis*(*out*)-[$RuCl_2$(Hbpp)(MeCN)(dmso)], **4**, as indicated in eqs 3 and 4. The formation of the same complex is also corroborated by cyclic voltammetric experiments (vide infra).

$$\underset{\textbf{2a}}{\textit{trans,cis}\text{-}[RuCl_2(Hbpp)(dmso)_2]} + MeCN \xrightarrow{h\nu} \underset{\textbf{4}}{\textit{cis}(\textit{out})\text{-}[RuCl_2(Hbpp)(MeCN)(dmso)]} + dmso \quad (3)$$

$$\underset{\textbf{2b}}{\textit{cis,cis}\text{-}[RuCl_2(Hbpp)(dmso)_2]} + MeCN \xrightarrow{h\nu} \underset{\textbf{4}}{\textit{cis}(\textit{out})\text{-}[RuCl_2(Hbpp)(MeCN)(dmso)]} + dmso \quad (4)$$

The kinetics of these substitution reactions display a pseudo-first-order dependence with regard to the desappearance of the starting complex (see Supporting Information).

The structural assignment of complex **4** is made on the basis of spectrophotometric, cyclic voltammetric, and NMR experiments together with the results already described in this paper and the data reported for related systems in the literature.[15,20b,21]

NMR spectroscopy clearly shows that in the photochemical reaction, when a solution of **2b** in acetonitrile-d_3 is irradiated, free dmso (δ 2.6 ppm) is generated. Redox potentials for complex **4** are also in agreement with the substitution of one dmso by one MeCN since the substitution of an anionic Cl ligand by a neutral MeCN would generate much higher redox potentials (vide infra).[22]

It is interesting to note here that for related systems namely the *cis,cis,trans*-[$RuCl_2$(*t*-py)$_2$(dmso)$_2$] (*t*-py, is 4-*tert*-buthylpyridine)[23] complex two successive substitutions of dmso for MeCN take place. In our case only one substitution is observed, suggesting that the hydrogen-bonded dmso is much more inert than the non-hydrogen-bonded one. These results reveal a high stability of the meridional positions occupied by the inner dmso and the coordinated nitrogen atoms of the Hbpp ligand.

Another interesting observation is that when the solvent of the final reaction is evaporated to dryness, a mixture of complex **4** and only **2b** is obtained irrespectively of the starting material. This clearly indicates that in **2b** there is a simple substitution of dmso by MeCN in the irradiation process whereas, in **2a**, as the substitution process takes place, a rapid rearrangement of one of Cl ligands is also occurring ending up in a cis-fashion. This is also in agreement with **2b** being thermodynamically more stable than **2a**.

Redox Chemistry and Linkage Isomerism. The redox properties of complexes described in this work have been investigated by cyclic voltammetric experiments which are shown in Figure 4 and in the Supporting Information.

The *cis*-Cl complex **2b** displays a chemically quasi-reversible wave for the Ru(III)/Ru(II) couple at $E_{1/2} = 0.840$ V vs SSCE ($E_{p,a} = 0.905$, $E_{p,c} = 0.78$, $\Delta E = 125$ mV) in neat acetonitrile solution containing 0.1 M TBAH. If a basic acetonitrile solution containing 0.1 M *t*-BuOK is used, then the wave shifts to lower potentials ($E_{1/2} = 0.425$ V, $E_{p,a} = 0.470$, $E_{p,c} = 0.380$, $\Delta E = 90$ mV) in agreement with the deprotonation of the pyrazolylic ring,[24]

$$\underset{\textbf{2b}}{\textit{cis,cis}\text{-}[RuCl_2(Hbpp)(dmso)_2]} + t\text{-}BuO^- \rightarrow \underset{\textbf{3b}}{\textit{cis,cis}\text{-}[RuCl_2(bpp)(dmso)_2]^-} + t\text{-}BuOH \quad (5)$$

A similar behavior is also observed for the *out*-MeCN species **4**, where under basic solutions the pyrazolyl ring is also deprotonated leading to *cis*(*out*)-[$RuCl_2$(bpp)(MeCN)-(dmso)]$^-$, **5**, which also has lower potentials (for **4**, $E_{1/2} =$

(21) Silva, D. O.; Saika, J. J.; Toma, H. E. *J. Photochem. Photobiol., A* **1998**, *112*, 209.
(22) Gerli, A.; Reedijk, J.; Lakin, M. T.; Spek, A. L. *Inorg. Chem.* **1995**, *34*, 1836.
(23) Silva, D. O.; Toma, H. E. *Can. J. Chem.* **1994,** *72*, 1705.
(24) Baitalik, S.; Flörke, U.; Nag, K. *Inorg. Chem.* **1999**, *38*, 3296.

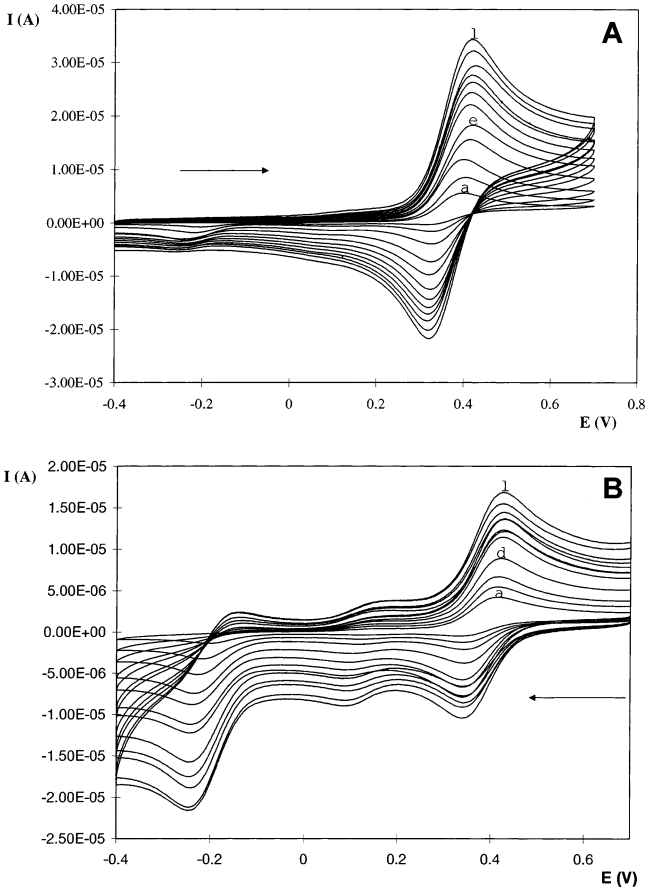

Figure 4. Cyclic voltammograms of 1 mM **3a** in an acetonitrile solution containing 0.1 M TBAH and ~4.5 × 10^{-3} M *t*-BuOK: (A) scanning anodically starting at −0.4 V at scan rates of (a) 20, (b) 50, (c) 100, (d) 200, (e) 300, (f) 400, (g) 500, (h) 600, (i) 700, (j) 800, (k) 900, and (l) 1000 mV/s; (B) scanning cathodically starting at 0.7 V at the same rates applying an equilibration time of 3 min. In both cases the initial scan direction is indicated with an arrow.

0.660 V, $E_{p,a} = 0.690$, $E_{p,c} = 0.630$, $\Delta E = 60$ mV; for **5,** $E_{1/2} = 0.130$ V, $E_{p,a} = 0.160$, $E_{p,c} = 0.100$, $\Delta E = 60$ mV).

For complex **3a**, the cyclic voltammograms displayed in Figure 4 clearly indicate the presence of linkage isomerism when the oxidation state three is reached.

With anodic scanning starting at −0.4 V, a single peak (i_{a1}) is observed associated with the Ru(III)/Ru(II) couple at $E_{1/2} = 0.380$ V vs SSCE ($E_{p,a} = 0.420$, $E_{p,c} = 0.340$, $\Delta E =$ 80 mV). In the reverse scan, the corresponding cathodic peak current (i_{c1}) becomes less intense and a new peak (i_{c2}) grows up at $E_{1/2} = -0.200$ V vs SSCE ($E_{p,a} = -0.155$, $E_{p,c} = -0.245$, $\Delta E = 90$ mV). This effect becomes very pronounced by staring at 0.7 V and scanning cathodically as can be observed in Figure 4B. The ratios of $[i_{c1}]/[i_{a1}]$ and $[i_{c2}]/[i_{a2}]$ are strongly dependent on the scan rates and are consistent with the involvement of chemical reactions coupled to electrochemical processes presented in Scheme 2. The dramatic change of $E_{1/2}$ from 0.380 to −0.200 V associated with the chemical reaction is analogous to those previously reported by Taube et al.[23] for S- and O-bound linkage isomers of $[Ru(NH_3)_5(dmso)]^{3+/2+}$ complex. By analogy to the literature,[23,25] the pair of anodic and cathodic peaks at −0.20 V are assigned to a single O-bound isomer in the *trans,cis*-

Scheme 2. Thermodynamic Cycle for the Linkage Isomerization Process That Takes Places during the Electrochemical Oxidation of Complex **3a**

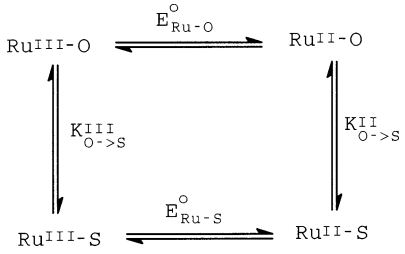

$[RuCl_2(Hbpp)(dmso)_2]$ complex, e.g.

$$Ru^{III}-O \underset{k^{III}_{S\to O}}{\overset{k^{III}_{O\to S}}{\rightleftharpoons}} Ru^{III}-S \quad K^{III}_{O\to S} \tag{6}$$

The equilibrium constant for the Ru(III)−O/Ru(III)−S reaction can be estimated from the cyclic voltammograms (Figure 4B) starting at 0.70 V with an equilibration time of 3 min to ensure its completeness. In the present case, $K^{III}_{O\to S}$ can be calculated from the plot of $[i_{c1}]/[i_{c2}]$ vs v^{-1} and extrapolating to $v \to \infty$; this gives a value of $K^{III}_{O\to S} = 0.255 \pm 0.025$. The kinetic isomerization constants were calculated from the working curves proposed by Shain et al.[26] for a reversible chemical reaction preceding an electron transfer (case III). The ratios i_k/i_d (i_k is the measured peak current; i_d is the corresponding diffusional current in the absence of a chemical reaction) were obtained from $[i_{c1}] = i_k$, starting at 0.7 V and from $[i_{a1}] = i_d$ starting at −0.4 V. This yields the following kinetic constants: $k^{III}_{O\to S} = 0.017$ s^{-1}; $k^{III}_{S\to O} = 0.065$ s^{-1}. On the basis of the equilibrium constant $K^{III}_{O\to S}$ and assuming that $E° = E_{1/2}$, the thermodynamic cycle shown in Scheme 2 can be built. This allows one to calculate $K^{II}_{O\to S}$, which turns out to be 6.45 × 10^9. $k^{II}_{O\to S}$ can be calculated from the dependence of $\ln(i_{a1}/v^{1/2})$ vs time,[23] which in this case was linear giving a rate constant of $k^{II}_{O\to S} = 0.132$ s^{-1}. With this value and $K^{II}_{O\to S}$ we obtain $k^{II}_{S\to O} = 2.1 \times 10^{-11}$ s^{-1}.

For the *trans*-Cl complex **3a**, Figure 4B shows the appearance of a new wave at 0.130 V on scanning cathodically presumably due to the formation of complex **5** (it has exactly the same potential as the one generated photochemically) through the substitution of a dmso ligand by the solvent. For the protonated *trans*-Cl isomer **2a**, the system becomes much more complex due to a number of decomposition products that are observed, besides the linkage isomerization process just described above, associated both with the electron-transfer processes and the equilibrium processes.

Catalysis. The catalytic properties of isomers **3a,b** were tested with regard to their aptitude to perform hydrogenation and hydrogen transfer type of reactions with carbonylic substrates. For the former reaction, acetophenone was used as substrate dissolved in 1,2-dichloroethane at 80 °C overnight with H_2 pressure of 40 atm. No reaction at all

(25) (a) Yeh, A.; Scott, N.; Taube, H. *Inorg. Chem.* **1982**, *21*, 2542. (b) Costa, G.; Balducci, G.; Alessio, E.; Tavagnacco, C.; Mestroni, G. *J. Electroanal. Chem.* **1990**, *296*, 57.
(26) Nicholson, R. S.; Shain, I. *Anal. Chem.* **1964**, *36*, 706.

occurred. Better results were obtained in the hydrogen transfer type of reaction for the hydrogenation of acetophenone using 2-propanol as the source of reducing equivalents.

$$\mathrm{PhC(O)Me} + \textit{i}\text{-PrOH} \xrightarrow{\mathrm{cat}} \mathrm{PhCH(OH)Me} + \mathrm{MeC(O)Me} \quad (7)$$

The system "1.40 mM **3a**/120 mM PhC(O)Me/50 mM *t*-BuOK/15 mM PhPh/solvent 2-propanol" at 80 °C yields 50.5 mM 2-phenylethyl alcohol as the only product, which represents a 42.1% conversion with regard to the original substrate concentration and 36.1 metal cycles. Under similar conditions the *cis*-Cl complex **3b** yields only 17.7 mM PhCH(OH)Me (14.8% conversion; 12.3 metal cycles) which manifests a clearly distinctive reactivity with regard to the isomer used as catalyst. Under conditions similar to the ones just described here, lowering the temperature to 298 K produces a drastic decrease of both catalyst activities yielding conversions lower than 7%.

The first step in the currently accepted mechanism for this reaction[27] is a ligand substitution process. This is in agreement with the results presented here since **2a** is thermodynamically less stable than **2b** and thus a substitution process should be easier in the former than in the latter. This is also in line with the photochemical reaction described in this work, where the substitution process occurs faster for **2a** than for **2b**.

(27) (a) Zassinovich, G.; Mestroni, G.; Gladiali, S. *Chem. Rev.* **1992**, *92*, 1051. (b) de Graauw, C. F.; Peters, J. A.; van Bekkum, H.; Huskens, J. *Synthesis* **1994**, 1007. (c) Schröder, D.; Schwarz, H. *Angew. Chem., Int. Ed. Engl.* **1990**, *29*, 910−912. (d) Morton, D.; Cole-Hamilton, D. J. *J. Chem. Soc., Chem. Commun.* **1988**, 1154. (e) Blum, O.; Milstein, D. *Angew. Chem., Int. Ed. Engl.* **1995**, *34*, 229. (f) Blum, O.; Milstein, D. *J. Am. Chem. Soc.* **1995**, *117*, 4582. (g) Aranyos, A.; Csjernyik, G.; Szabó, K. J.; Bäckvall, J.-E. *Chem. Commun.* **1999**, 351. (h) Zhao, J.; Hesslink, H.; Hartwig, J. F. *J. Am. Chem. Soc.* **2001**, *123*, 7220. (i) Sasson, Y.; Blum, J. *J. Chem. Soc., Chem. Commun.* **1974**, 309. (j) Thorn, D. L.; Hoffmann, R. *J. Am. Chem. Soc.* **1978**, *100*, 2079. (k) Koga, N.; Morokuma, K. *Chem. Rev.* **1991**, *91*, 823. (l) Noyori, R.; Yamakawa, M.; Hashiguchi, S. *J. Org. Chem.* **2001**, *66*, 7931.

In summary, the physical and chemical properties of two new complexes, **2a,b,** containing the dinucleating ligand Hbpp are fully reported. Hydrogen bonding between one of the dmso ligands and the pyrazolylic ring has proven to be a key factor that allows one to understand and rationalize a significant part of their chemistry, namely, the following: (a) the transformation of complex **2a** mainly into **2b** with insignificant amounts of the other possible isomers; (b) structurally, the low angle between the inner dmso ligand with regard to the Hbpp ligand in **2a**; (c) the smooth photochemical substitution of only one dmso ligand by acetonitrile and its reverse reaction. Electrochemical experiments via CV enables one to quantitatively describe the interesting Ru−dmso linkage isomerization processes (Ru−S/Ru−O) that take place associated with electron-transfer processes for the *trans*-Cl **3a** isomer. In sharp contrast the *cis*-Cl **3b** isomer and its one-electron oxidation products are chemically stable. Finally, also remarkable is the distinctive ability of **3a** to act as a catalyst in a quite efficient manner as compared to **3b** in hydrogen transfer reactions.

Acknowledgment. This research has been financed by the MCYT of Spain through Project BQU2000-0458. A.L. is grateful to the CIRIT Generalitat de Catalunya (Spain) for the Distinction Award and the Aid SGR2001-UG-291. A.L. also thanks Johnson and Matthey for a $RuCl_3 \cdot xH_2O$ loan. C.S. is grateful for the award of a doctoral grant from the CIRIT. Prof. E. Toma, from Universidade de Sao Paulo, is gratefully acknowledged for helpful electrochemical discussions.

Supporting Information Available: Additional data related to spectroscopic (NMR, UV−vis) and electrochemical properties (CV) for the complexes described in this work and CIF files containing all crystallographic information for complex **2a** (CCDC No. 204507) and **2b** (CCDC No. 204508). This material is available free of charge via Internet at http://pubs.acs.org.

IC026114O